JOURNAL OF SOLID STATE CHEMISTRY **126,** 242–252 (1996)
ARTICLE NO. 0335

Surface and Bulk Properties of Stoichiometric and Nonstoichiometric Strontium Hydroxyapatite and the Oxidation of Methane

Shigeru Sugiyama,[1] Toshimitsu Minami, Hiromu Hayashi, Michie Tanaka,[+] and John B. Moffat[++]

Department of Chemical Science and Technology, Faculty of Engineering, The University of Tokushima, Minamijosanjima, Tokushima, 770 Japan; [+]Shikoku Research Institute Inc., 2109 Yashima-nishi, Takamatsu, 761–01 Japan; and [++]Department of Chemistry and the Guelph-Waterloo Centre for Graduate Work in Chemistry, University of Waterloo, Waterloo, Ontario, Canada N2L 3G1

Received March 28, 1996; accepted August 1, 1996

The oxidation of methane on near-stoichiometric strontium hydroxyapatites pretreated at 873, 1048 and 1123 K in O_2 has been examined in the presence and absence of tetrachloromethane (TCM) as a gas-phase additive at 973 K. Under these conditions, strontium hydroxyapatite, regardless of its stoichiometry, is converted, at least in part, to $Sr_3(PO_4)_2$. On introduction of TCM to the feedstream, the selectivities to carbon monoxide, ethane, and ethylene are increased while the conversion of methane is decreased. Qualitatively similar effects of TCM on the oxidation were observed on $Sr_3(PO_4)_2$ prepared by an independent procedure. Strontium chlorapatite, formed from the apatites and phosphate during the oxidation in the presence of TCM, as shown from XRD, contributes to the increased selectivity to CO and decreased conversion of methane.

INTRODUCTION

During the past decade a multitude of reports has appeared on the partial oxidation and oxidative coupling of methane and heterogeneous catalysts for these processes (1–6). Although considerable progress has been made in understanding the mechanisms of these catalyzed processes, industrial implementation has been retarded at least in part because of the oxidative instability of the value-added products. For these and other reasons, more recent attention has focused on the production of synthesis gas from methane for which a number of catalysts have been suggested (7–9).

The effects of the introduction of small quantities (<1 mole%) of tetrachloromethane (TCM) as a gas phase additive in the feedstream for the partial oxidation and oxidative coupling of methane have been studied in our laboratories with a wide variety of heterogeneous catalysts (10–20). Although with the latter process the enhancement of the conversion of methane and the selectivities to C_{2+} hydrocarbons are generally obtained, recent results show that on stoichiometric and nonstoichiometric calcium hydroxyapatites the selectivities to carbon monoxide were increased (18–20).

Calcium hydroxyapatites $[Ca_{10-z}(HPO_4)_z(PO_4)_{6-z}(OH)_{2-z}; 0 \leq Z \leq 1]$ are bifunctional catalysts, with acidic or basic properties, depending on their compositions (21–26). Recently, calcium (27, 28), strontium (29), and lead–calcium (30–32) hydroxyapatites have been studied in our laboratories as catalysts for the conversion of methane in the absence of TCM. Lead–calcium hydroxyapatites were found to catalyze the selective coupling (30–32) while with calcium (27, 28) and strontium (29) hydroxyapatites the principal products are carbon oxides.

In view of the marked effect of the nature of the cations in hydroxyapatite on the products generated from methane, extension of the previous work to include strontium as the cation appeared to be warranted. In the present study, the introduction of a small partial pressure of TCM into the feedstream of the methane oxidation is shown to produce a substantial increase in the selectivity to CO as well as to C_{2+} hydrocarbons on nonstoichiometric strontium hydroxyapatites [stoichiometric form; $Sr_{10}(PO_4)_6(OH)_2$] under the same reaction and pretreatment conditions as those employed in our previous studies on the methane oxidation over calcium hydroxyapatites (18–20). Furthermore, the effects of the pretreatment temperatures of the apatites on their oxidation and thermal stabilities have been examined together with that of the space time on the oxidation of methane in the presence and absence of TCM over $Sr_3(PO_4)_2$.

[1] To whom correspondence should be addressed.

0022-4596/96 $18.00

TABLE 1
Surface Areas and Apparent Densities of Fresh Catalysts

Catalyst	$SrHAp_{1.61}$	$SrHAp_{1.67}$	$SrHAp_{1.70}$	$SrHAp_{1.73}$	$Sr_3(PO_4)_2$
Surface area[a]	72.4	60.3	67.9	65.5	0.7
Density[b]	0.42	0.45	0.40	0.43	1.27

[a] BET surface area (m^2/g).
[b] Apparent density (g/cm^3).

EXPERIMENTAL

Catalysts

Strontium hydroxyapatites ($SrHAp_{1.73}$,$SrHAp_{1.70}$, $SrHAp_{1.67}$, and $SrHAp_{1.61}$), where the subscripts represent the Sr/P atomic ratio of each apatite, were prepared (29) from $Sr(NO_3)_2$ (Wako Pure Chemicals, Osaka) and $(NH_4)_2HPO_4$ (Wako) applying the procedure reported by Hayek and Newesely for that of calcium hydroxyapatite (33). The resulting solids were calcined at 773 K for 3 h after drying at 373 K overnight.

Strontium phosphate was prepared by heating $SrCO_3$ (Wako) and pyrophosphate ($Sr_2P_2O_7$) together in a molar ratio of 1:1 at 1173 K for 15 h in air (34, 35). The pyrophosphate was prepared by slow addition, while stirring, of $Sr(OH)_2 \cdot 8H_2O$ (Wako) to a solution of 25 ml of 85% H_3PO_4 (Wako) per 500 ml of water, until a small amount of solid remained undissolved. The excess hydroxide was removed by filtration and the filtrate was slowly heated and rapidly stirred. At about 313 K, a very fine precipitate began to form and the precipitation was nearly complete at 353 K. The precipitate was filtered, washed with boiled water, methanol, and diethyl ether, dried at room temperature overnight (35, 36), and heated at 1173 K for 13 h (27, 35).

Particles of 0.35–1.75 mm were employed in the present study.

Apparatus and Procedure

The catalytic experiments were performed in a fixed-bed continuous-flow quartz reactor operated at atmospheric

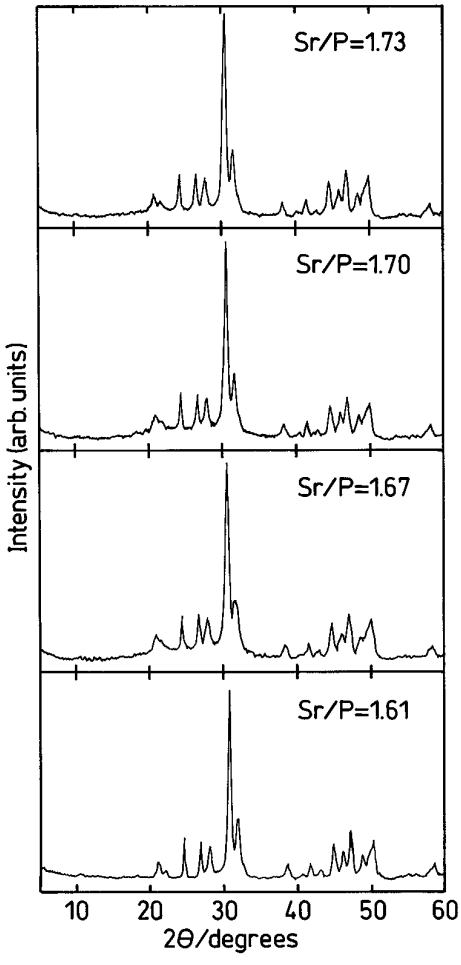

FIG. 1. XRD patterns of the fresh strontium hydroxyapatites.

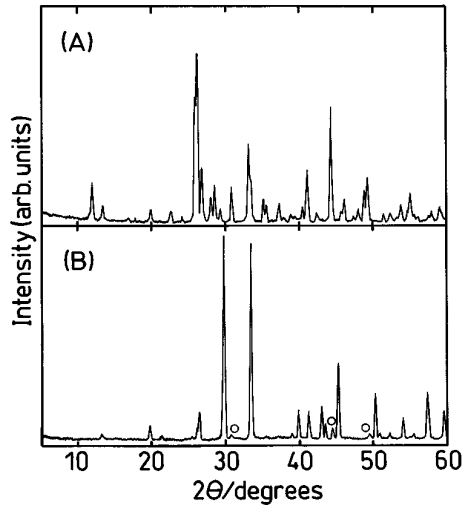

FIG. 2. XRD patterns of synthesized $Sr_2P_2O_7$ (A) and $Sr_3(PO_4)_2$ (B). Open circle; unidentified peak.

TABLE 2
Binding Energies and Atomic Ratios of the Fresh Catalysts

Catalyst	Time[a] min	Binding energy/eV				Atomic ratio	
		Sr $3p_{3/2}$	Sr $3p_{1/2}$	O 1*s*	P 2*p*	Sr/P	O/Sr
$SrHAp_{1.61}$	0	269.3	279.5	531.4	190.8	1.67	1.88
	1	269.8	280.1	531.7	191.1	1.94	1.79
$SrHAp_{1.67}$	0	268.9	279.2	530.9	190.3	1.53	1.70
	1	269.7	280.0	531.6	190.8	1.87	1.94
$SrHAp_{1.70}$	0	268.9	279.3	531.1	190.6	1.67	2.02
	1	269.5	279.9	531.6	190.7	1.87	2.05
$SrHAp_{1.73}$	0	269.0	279.0	530.9	190.3	1.61	2.30
	1	269.5	280.0	531.3	191.0	1.84	2.29
$Sr_3(PO_4)_2$	0	267.8	278.4	529.8	188.9	1.63	2.14
	1	268.2	278.7	530.0	189.5	1.90	1.93

[a] Etching time.

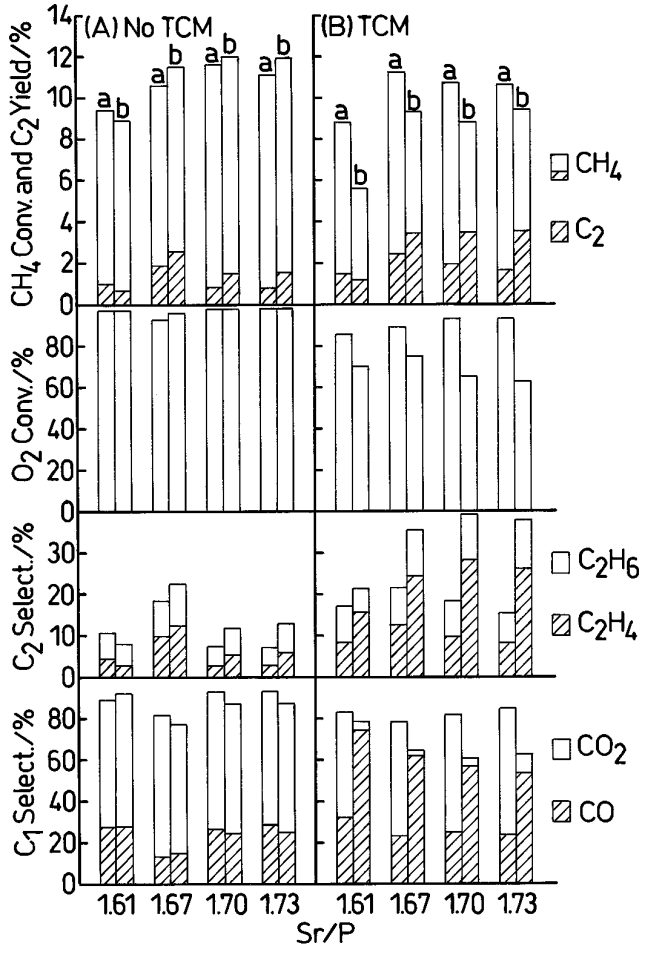

FIG. 3. The effects of the Sr/P ratio of strontium hydroxyapatites on the oxidation of methane at 973 K in the absence (A) and presence (P) of TCM. a, 0.5 h on-stream; b, 6 h on stream. Catalysts were pretreated at 1048 K in O_2 (25 ml/min) for 1 h. Reaction conditions: W = 0.5 g, F = 30 ml/min, $P(CH_4)$ = 28.7 kPa, $P(O_2)$ = 4.1 kPa, and P(TCM) = 0 or 0.17 kPa diluted with He.

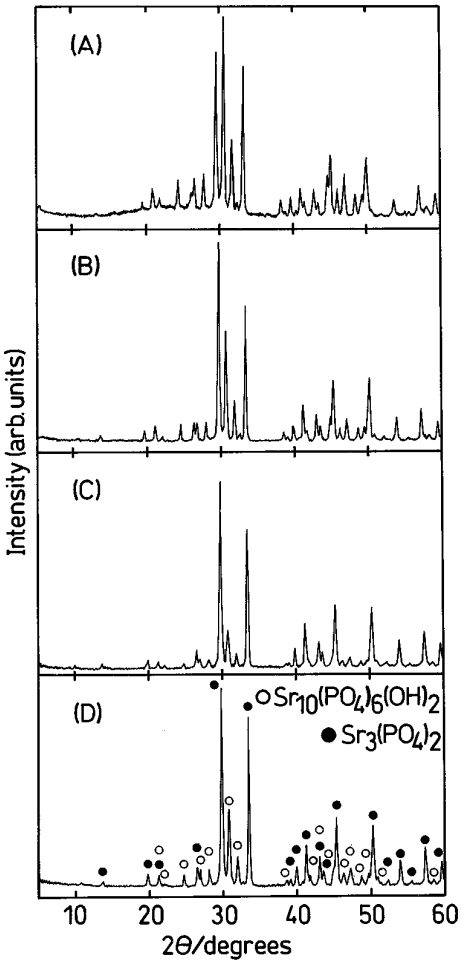

FIG. 4. XRD patterns of the catalysts (previously employed in obtaining results reported in Fig. 3A but after 6 h on stream) used in the oxidation of methane in the absence of TCM. (A) $SrHAp_{1.73}$, (B) $SrHAp_{1.70}$, (C) $SrHAp_{1.67}$, (D) $SrHAp_{1.61}$.

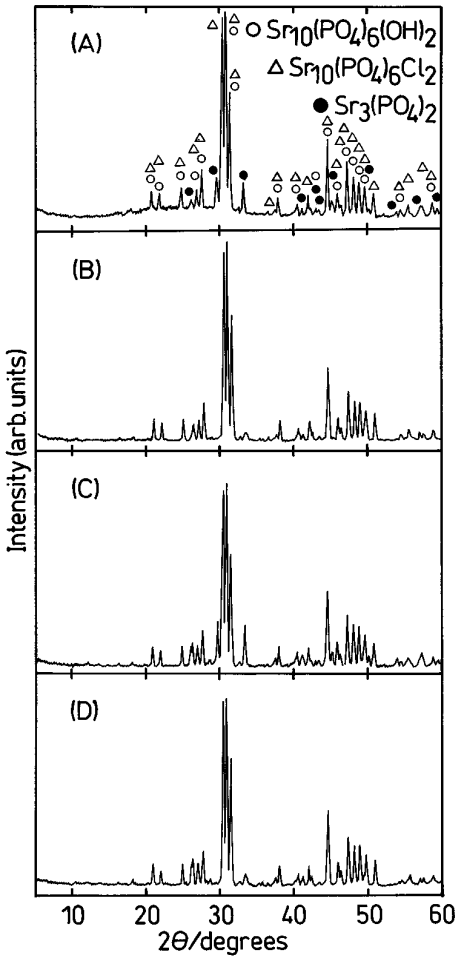

FIG. 5. XRD patterns of the catalysts (previously employed in obtaining results reported in Fig. 3B but after 6 h on stream) used in the oxidation of methane in the presence of TCM. (A) $SrHAp_{1.73}$, (B) $SrHAp_{1.70}$, (C) $SrHAp_{1.67}$, (D) $SrHAp_{1.61}$.

pressure. Details of the reactor design and catalyst packing procedure have been described elsewhere (12). Prior to reaction the catalyst was pretreated *in situ* in an oxygen flow (25 ml/min) at 873, 1048, or 1123 K for 1 h. The reaction conditions were as follows: $W = 0.5$ g, $F = 30$ ml/min, $T = 973$ K, $P(CH_4) = 28.7$ kPa, $P(O_2) = 4.1$ kPa, and $P(TCM) = 0$ or 0.17 kPa; the balance to atmospheric pressure was provided by helium.

Analysis and Characterization

The reactants and products were analyzed with an on-stream gas chromatograph (Shimadzu GC-8APT) equipped with a TC detector and integrator (Shimadzu C-R6A). The columns used in the present study and the methods employed in the calculation of conversions and selectivities have been described previously (12).

The surface areas were measured with a conventional BET nitrogen adsorption apparatus (Shibata P-700).

Powder X-ray diffraction (XRD) patterns were recorded with a CN-2011 (Rigaku) diffractometer, using monochromatized Cu$K\alpha$ radiation. Patterns were recorded over the range $2\theta = 5°$–$60°$.

X-ray photoelectron spectroscopy (XPS) (Shimadzu ESCA-1000AX) employed monochromatized Mg$K\alpha$ radiation. The binding energies were corrected using 285 eV for C 1*s* as an internal standard. Argon-ion etching of the catalyst was carried out at 2 kV for 1 min with a sputtering rate estimated as ca. 2 nm/min for SiO_2.

The concentrations of Sr and P or C1 in each catalyst were determined in aqueous HNO_3 solution by inductively coupled plasma (ICP) spectrometry (ICPS-5000, Shimadzu) or ion-chromatography (IC7000S, Yokokawa).

RESULTS AND DISCUSSION

Properties of Catalysts

The BET surface areas and bulk densities of SrHAp and $Sr_3(PO_4)_2$ are summarized in Table 1. The XRD pat-

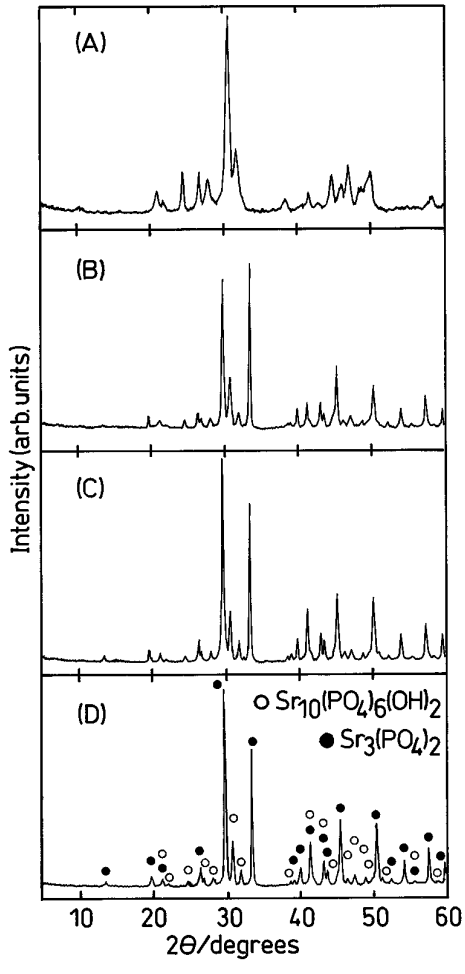

FIG. 6. XRD patterns of $SrHAp_{1.67}$ pretreated at different temperatures. Pretreatment temperatures: (A) 873 K, (B) 973 K, (C) 1048 K, and (D) 1123 K. Pretreatment conditions: 25ml/min of O_2 for 1 h.

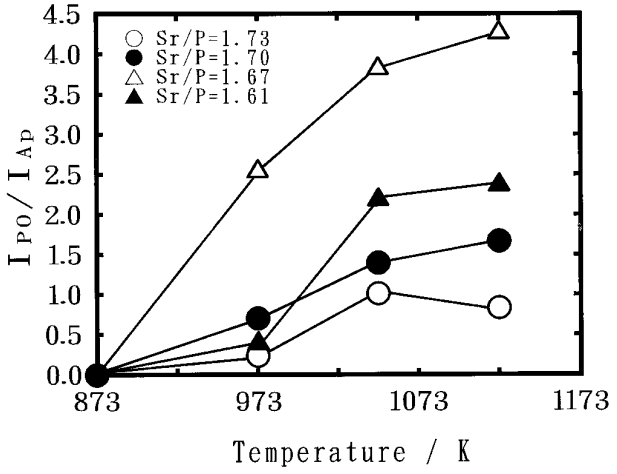

FIG. 7. Relative XRD intensities of I_{PO}/I_{AP} in SrHAp pretreated at different temperatures. I_{PO}, intensity of $Sr_3(PO_4)_2$ at $2\theta = 29.6°$. I_{AP}, intensity of $Sr_{10}(PO_4)_6(OH)_2$ at $2\theta = 30.5°$. Pretreatment conditions: same as those in Fig. 6.

terns (Fig. 1) of the four samples of SrHAp with Sr/P values of 1.61, 1.67 (stoichiometric composition), 1.70, and 1.73 are essentially indistinguishable, as similarly found with calcium hydroxyapatites (19, 38), and are matched with that of $Sr_{10}(PO_4)_6(OH)_2$, as provided in JCPDS 33–1348, although some evidence of noncrystallinity is evident. Figure 2 shows XRD patterns of $Sr_2P_2O_7$ (A) employed as an intermediate in the synthesis of the phosphate and $Sr_3(PO_4)_2$ (B) which are matched with JCPDS 24–1011 for (A) and JCPDS 24–1008 for (B). Unidentified trace signals seen in (B) are expected to be due to $Sr_{10}(PO_4)_6(OH)_2$. XPS analyses of the fresh SrHAp show no significant variation with composition of the Sr $2p_{1/2}$ and $2p_{3/2}$, P $2p$, and O $1s$ binding energies either before or after argon-ion etching, but those on $Sr_3(PO_4)_2$ were somewhat smaller than those on the various SrHAp (Table 2). No significant shoulders were observed in any of the spectra. The Sr/P atomic ratios obtained from XPS for the fresh SrHAp were not identical to those of the bulk phase.

Oxidation of Methane on SrHAp

The oxidation of methane on SrHAp was first examined at the reaction and pretreatment temperatures (973 and 1048 K, respectively) previously employed with calcium hydroxyapatites (CaHAp) (18–20) (Fig. 3). In the absence of TCM, the conversion of methane changes relatively little with Sr/P. While the selectivity to C_2 compounds reaches a maximum on $SrHAp_{1.67}$, that to carbon monoxide is at a minimum regardless of time-on-stream. Although these observations are qualitatively similar to those on CaHAp (19), the conversions of methane on SrHAp are larger than those on CaHAp and the deep oxidation to carbon dioxide proceeds more easily on SrHAp than on CaHAp. In the presence of TCM, the conversion of methane on $SrHAp_{1.61}$ decreases markedly with increasing time-on-stream but less so for those catalysts where Sr/P > 1.61, as observed on CaHAp (19). With all SrHAp compositions, however, the C_2 selectivities and particularly those to C_2H_4 are increased on addition of TCM and most noticeably after 6 h on stream. These observations are distinctly different from those on CaHAp (19). In contrast, the selectivities to CO_x decrease in the presence of TCM although those to CO after 6 h on stream have increased for all compositions.

The evident dissimilarity of the results obtained previously with CaHAp (18–20) as compared with the present results for SrHAp suggest that composition and structure, particularly that related to the nature of the cation, are of considerable importance. To provide further information

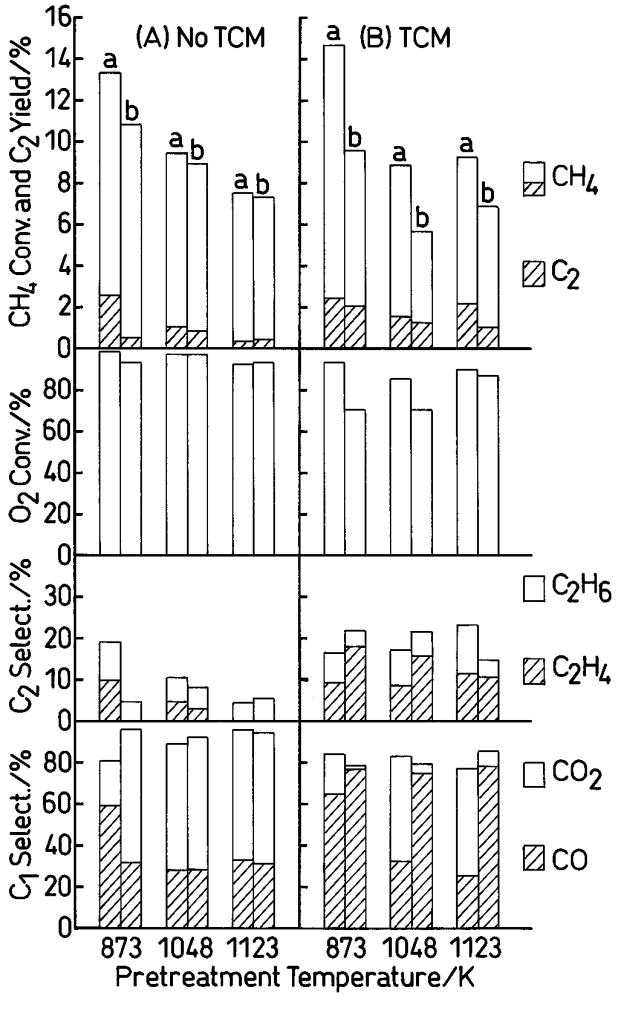

FIG. 8. Effects of the pretreatment temperature on the oxidation of methane in the absence (A) and presence (B) of TCM on $SrHAp_{1.61}$ at 973 K. a, 0.5 h on stream; b, 6 h on stream. Catalysts were pretreated at 873, 1048, or 1123 K in O_2 (25 ml/min) for 1 h. Reaction conditions: same as those in Fig. 3.

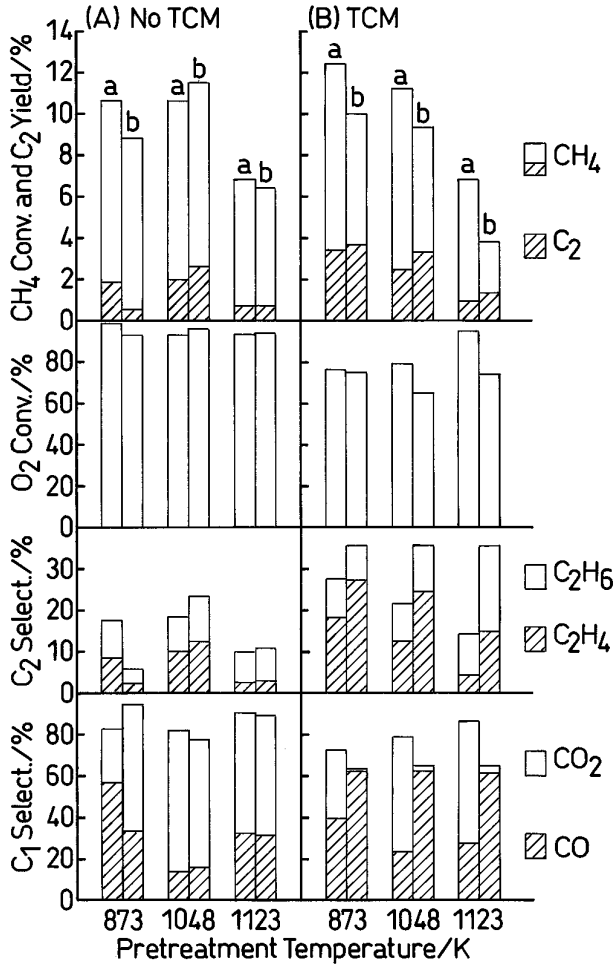

FIG. 9. Effects of the pretreatment temperature on the oxidation of methane in the absence (A) and presence (B) of TCM on $SrHAp_{1.67}$ at 973 K. a, 0.5 h on stream; b, 6 h on stream. Pretreatment and reaction conditions: same as those in Fig. 8.

on the bulk structural properties, XRD data for the catalysts after use in the conversion of methane with and without TCM have been obtained (Figs. 4 and 5). The XRD patterns of the catalysts employed in the conversion of methane without added TCM show that a substantial portion of the SrHAp, the extent of which is dependent upon the Sr/P ratio, is converted to $Sr_3(PO_4)_2$ during the reaction (Fig. 4). Where TCM was present during the methane conversion, XRD of the resulting SrHAp catalysts provided evidence for the formation of both strontium chlorapatite [$Sr_{10}(PO_4)_6Cl_2$] and $Sr_3(PO_4)_2$, with the quantities of these again dependent on Sr/P (Fig. 5). The present results suggest that the conversion of SrHAp to $Sr_3(PO_4)_2$ occurs at a temperature of 1048 K or lower, although the presence of methane and its oxidation products introduces an additional factor. In contrast, one recent report suggests that SrHAp is thermally stable to 1123 K (39) while another suggests that SrHAp is stable at 873 K but substantially converted to the phosphate at 1073 K (29). To provide further information XRD patterns of $SrHAp_{1.67}$ after pretreatment at various temperatures have been obtained (Fig. 6). The aliquot pretreated at 873 K showed only XRD peaks attributed to strontium hydroxyapatite, the most intense of which appeared at a 2θ value of 30.5°, assigned to (211) and (112) planes of $Sr_{10}(PO_4)_6(OH)_2$ [JCPDS 33–1348]. However, the patterns of samples pretreated at higher temperatures contained additional XRD peaks, which increased with pretreatment temperatures, the most intense of which appeared at 29.6° and 33.2°, assigned to (015) and (110) planes, respectively, of $Sr_3(PO_4)_2$ [JCPDS24–1008].

To illustrate both compositional and temperature effects on the apatite to phosphate process the relative intensity

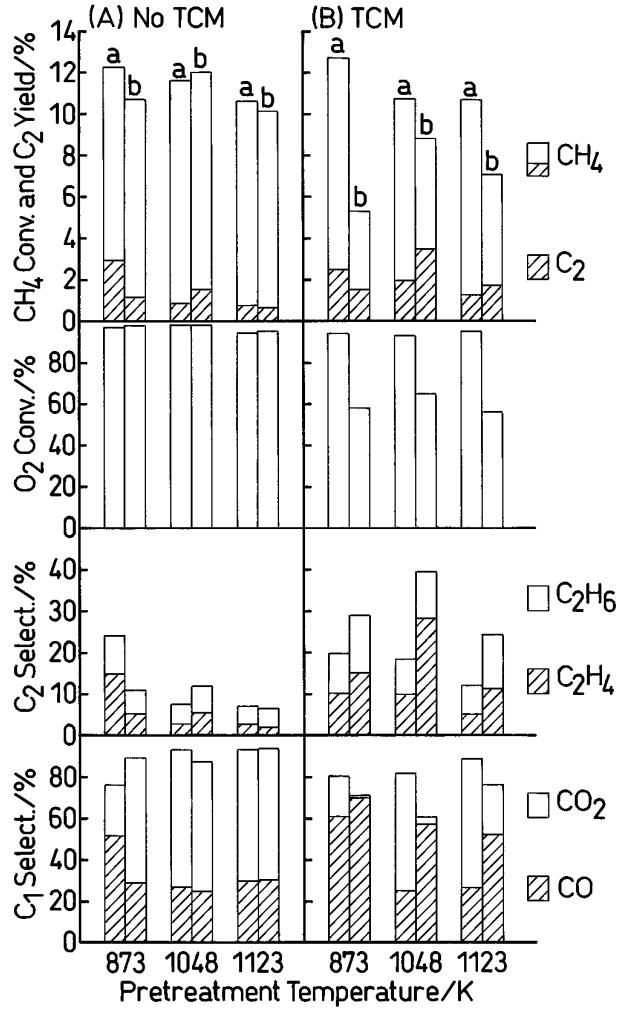

FIG. 10. Effects of the pretreatment temperature on the oxidation of methane in the absence (A) and presence (B) of TCM on $SrHAp_{1.70}$ at 973 K. a, 0.5 h on stream; b, 6 h on stream. Pretreatment and reaction conditions: same as those in Fig. 8.

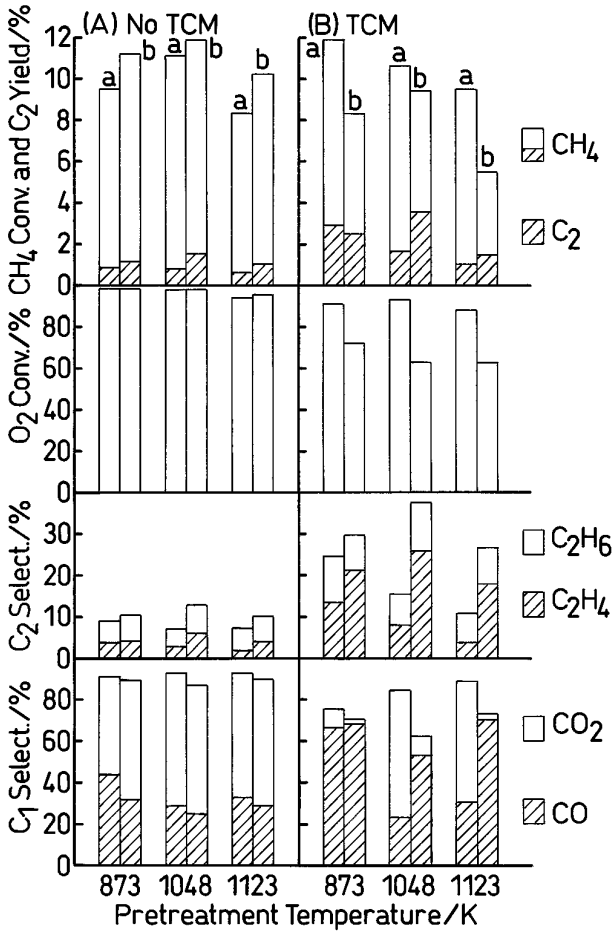

FIG. 11. Effects of the pretreatment temperature on the oxidation of methane in the absence (A) and presence (B) of TCM on $SrHAp_{1.73}$ at 973 K. a, 0.5 h on stream; b, 6 h on stream. Pretreatment and reaction conditions: same as those in Fig. 8.

of the I_{PO}/I_{AP} signals of each apatite and for each temperature are shown in Fig. 7, where I_{PO} and I_{AP} represent the intensity of the 30.5° signal due to the apatite and that of the 29.6° signal of $Sr_3(PO_4)_2$, respectively. It is evident that the conversion of the apatite to the phosphate occurs at temperatures as low as 973 K and possibly lower, for all compositions examined, but particularly with the stoichiometric apatite. It is of interest to compare the present results with those reported earlier for CaHAp. One set of workers has found that after heating at 973 K (40) or after use in the oxidation of methane at 1073 K, CaHAp remains as the apatite while others have shown that stoichiometric and nonstoichiometric CaHAp is stable up to 1023 K (41). Evidently, calcium hydroxyapatite has higher stability, apparently both kinetic and thermodynamic, with respect to the conversion to the phosphate, than strontium hydroxyapatite.

Effects of Pretreatment Temperature

To examine the role of $Sr_3(PO_4)_2$ in the methane oxidation reaction, aliquots of each of the SrHAp compositions were pretreated at different temperatures prior to their use in the methane reaction (Figs. 8–11). In the absence of TCM the conversion decreased with increasing pretreatment temperature with $SrHAp_{1.61}$ (Fig. 8A) but showed relatively little dependence on temperature with the remaining catalysts (Figs. 9–11A). Although, in the absence of TCM, the effects of the pretreatment temperature on the selectivities were dependent upon Sr/P (Figs. 8–11A), the results obtained for the 1.61, 1.67, and 1.70 Sr/P compositions pretreated at 873 K were quite similar. XRD patterns of the catalysts previously employed in the methane reaction (without TCM) at 973 K after 6 h on stream show that, except for the 1.61 Sr/P composition, the conversion to the phosphate is independent of the pretreatment temperature for 873–1123 K (Table 3), with the amounts of the phosphate formed being relatively large and similar to those found after pretreatment of the fresh catalysts at 1123 K. The exceptionally small quantity of phosphate formed with the 1.61 Sr/P composition pretreated at 873 K is of particular interest (Table 3).

In view of the absence of any correlation between the conversions and selectivities in the absence of TCM and the quantities of phosphate formed, XPS analyses were carried out to provide further information. Although no peaks other than those observed with the fresh catalysts were detected on the used catalysts, the Sr/P and O/Sr ratios were found to depend on the pretreatment conditions (Table 4). With the exception of the 1.61 composition, the O/Sr values were at a minimum for the used catalysts pretreated at 1048 K while the conversion of methane at 6 h on stream was at a maximum at this pretreatment temperature (Table 4 and Figs. 9–11A). The dissimilar catalytic behavior of the 1.61 composition in comparison with the stoichiometric and greater than stoichiometric catalysts, the latter three of which possess similar catalytic properties, is somewhat reminiscent of the observations for the nonstoichiometric ($Ca/P < 1.67$) and stoichiometric ($Ca/P = 1.67$) calcium hydroxyapatites (21–26).

In the presence of TCM certain similarities in the reaction results, not seen where TCM was absent, are evident. The conversion decreased with increase in pretreatment temperature and particularly with time-on-stream (tos) (Figs. 8–11B). For each composition and pretreatment temperature the selectivity to CO increased with time-on-stream in the presence of TCM, at least in some cases more than doubling. In fact, after 6 h on stream, virtually all of the CO_x was CO with relatively little CO_2 being produced. In addition, the selectivity to C_2 compounds is generally enhanced where TCM is present and particularly so after 6 h on stream, in contrast with the results obtained with CaHAp.

TABLE 3
Relative Intensities of I_{PO}/I_{AP}[a] of SrHAp[b]

Temp.[c]	$SrHAp_{1.61}$	$SrHAp_{1.67}$	$SrHAp_{1.70}$	$SrHAp_{1.73}$
873	0.12	4.66	1.81	0.92
1048	2.48	4.62	1.77	0.83
1123	2.65	4.70	1.89	0.99

[a] I_{PO}; intensity of $Sr_3(PO_4)_2$ at $2\theta = 29.6°$. I_{AP}; intensity of $Sr_{10}(PO_4)_6(OH)_2$ at $2\theta = 30.5°$.
[b] Previously employed in obtaining results reported in Figs. 8–11A but after 6 h on stream.
[c] Pretreatment temperature (K).

TABLE 4
Atomic Ratio of Sr/P and O/Sr in the Near-Surface Region of SrHAp[a]

	$SrHAp_{1.61}$		$SrHAp_{1.67}$		$SrHAp_{1.70}$		$SrHAp_{1.73}$	
Temp.[b]	Sr/P	O/Sr	Sr/P	O/Sr	Sr/P	O/Sr	Sr/P	O/Sr
873	1.56	2.43	1.63	2.52	1.92	2.18	1.74	2.31
	(1.98)	(2.29)	(1.83)	(2.32)	(1.87)	(2.16)	(2.01)	(2.25)
1048	1.58	1.68	1.77	2.14	1.78	2.17	1.51	1.42
	(1.52)	(1.82)	(1.90)	(2.08)	(2.08)	(2.06)	(1.71)	(1.48)
1123	1.77	2.30	1.77	2.32	1.91	2.35	1.67	2.35
	(1.96)	(2.13)	(1.80)	(2.19)	(1.85)	(2.32)	(1.97)	(2.27)

Note. Values in parentheses are after argon-ion etching for 1 min.
[a] Previously employed in obtaining results reported in Figs. 8–11A but after 6 h on stream.
[b] The pretreatment temperature (K).

TABLE 5
Relative XRD Intensities (I_{AP}/I_{CI} and I_{PO}/I_{CI})[a] and CI/Sr Atomic Ratios of SrHAp[b]

	$SrHAp_{1.61}$			$SrHAp_{1.67}$			$SrHAp_{1.70}$			$SrHAp_{1.73}$		
	873	1048	1123	873	1048	1123	873	1048	1123	873	1048	1123
I_{Ap}/I_{CI}[a]	0.04	0.07	0.09	0.05	0.09	0.05	0.09	0.10	0.05	0.03	0.08	0.08
I_{PO}/I_{Cl}	0	0.05	0.03	0.40	0.27	1.21	0.19	0	1.74	0	0.23	0
Cl/Sr	0.20	0.20	0.20	0.14	0.15	0.08	0.16	0.17	0.09	0.18	0.16	0.19

[a] I_{PO}, intensity of $Sr_3(PO_4)_2$ at $2\theta = 29.6°$. I_{AP}, intensity of $Sr_{10}(PO_4)_6(OH)_2$ at $2\theta = 30.5°$. I_{Cl}, intensity of $Sr_{10}(PO_4)_6Cl_2$ at $2\theta = 30.3°$.
[b] Previously employed in obtaining results reported in Figs. 8–11B but after 6 h on stream.

Strontium chlorapatite appears as the principal component in the XRD patterns of the catalysts previously employed in the oxidation (TCM present, 6 h tos) of methane (Table 5). In catalysts of composition 1.67 and 1.70 previously employed in the methane reaction after pretreatment at 1123 K, the quantities of the chlorapatite are reduced while those of $Sr_3(PO_4)_2$ are increased, the former being confirmed by ion chromatography (Table 5).

The XPS analyses of the used samples showed no peaks other than those found for the fresh samples, except for that of Cl 2*p* at approximately 199 eV (Table 6). The Sr/P, O/Sr, and Cl/Sr ratios, although dependent on the pretreatment temperatures, showed no obvious correlation with the results from methane conversion in the presence of TCM. Although the XRD results showed that chlorapatite was the principal component of the catalysts employed in the reaction where TCM was present and thus that chlorapatite has a substantial influence on the reaction, the

TABLE 6
Sr/P, O/Sr, and Cl/Sr Atomic Ratios in the Near-Surface Region of SrHAp[a]

	873			1048			1123		
Temp.[b]	Sr/P	O/Sr	Cl/Sr	Sr/P	O/Sr	Cl/Sr	Sr/P	O/Sr	Cl/Sr
$SrHAp_{1.61}$	1.72	1.97	0.31	1.81	1.68	0.28	1.77	2.01	0.28
	(1.79)	(1.90)	(0.19)	(1.85)	(1.80)	(0.20)	(1.94)	(1.99)	(0.19)
$SrHAp_{1.67}$	1.69	2.09	0.21	1.59	2.24	0.23	1.65	2.09	0.14
	(1.91)	(2.02)	(0.15)	(1.70)	(2.04)	0.17	(1.77)	(1.84)	(0.13)
$SrHAp_{1.70}$	1.63	2.08	0.23	1.73	2.24	0.27	1.73	2.21	0.12
	(2.02)	(1.80)	(0.18)	(1.87)	(2.10)	(0.24)	(1.89)	(2.07)	(0.11)
$SrHAp_{1.73}$	1.70	2.09	0.28	1.59	2.14	0.24	1.85	1.93	0.29
	(1.89)	(2.00)	(0.19)	(1.62)	(1.89)	(0.19)	(1.83)	(1.89)	(0.21)

Note. Values in parentheses are after argon-ion etching for 1 min.
[a] Previously employed in obtaining results reported in Figs. 8–11B after 6 h on stream.
[b] The pretreatment temperature (K).

participation of $Sr_3(PO_4)_2$, which is formed from SrHAp during the pretreatment and reaction, cannot be disregarded.

Oxidation of Methane on $Sr_3(PO_4)_2$

In comparison with the SrHAp compositions, the conversions of methane on $Sr_3(PO_4)_2$ in the absence of TCM is significantly smaller as is the selectivity to C_2H_4, while the selectivities to CO and CO_2 are similar (Fig. 12). This appears to be at least qualitatively similar to the results shown in Figs. 8–10A for the SrHAp compositions where, with the exception of the 1.73 composition, the conversion of methane decreased with time-on-stream and the content of $Sr_3(PO_4)_2$ increased. On introduction of TCM into the feedstream, the conversion of methane on $Sr_3(PO_4)_2$ after 0.5 h on stream increased for all *W*/*F* but after 6 h on stream had decreased to approximately the same values found when TCM was not present. The selectivity to C_2H_4 increased on addition of TCM at the two lower values of *W*/*F* and remained little changed with time-on-stream. However, with the highest *W*/*F*, the selectivity to C_2H_4 attained values similar to those found with the two lower values of *W*/*F* only after 6 h on stream. Somewhat similar behavior of the selectivity to CO was observed. With the two lowest *W*/*F*, the selectivity to CO increased on addition of TCM while CO_2 vanished with little or no changes after 6 h on stream. As before, with the highest *W*/*F*, the selectivity to CO was initially low, comprising approximately 25% of the CO_x content, but increased after 6 h on stream to a value similar to that obtained at the two lower values of *W*/*F*.

The XRD patterns of $Sr_3(PO_4)_2$ after use in the methane reaction at the lowest and highest values of *W*/*F* show that the phosphate can be converted to chlorapatite when TCM is present, the extent of such conversion being higher at

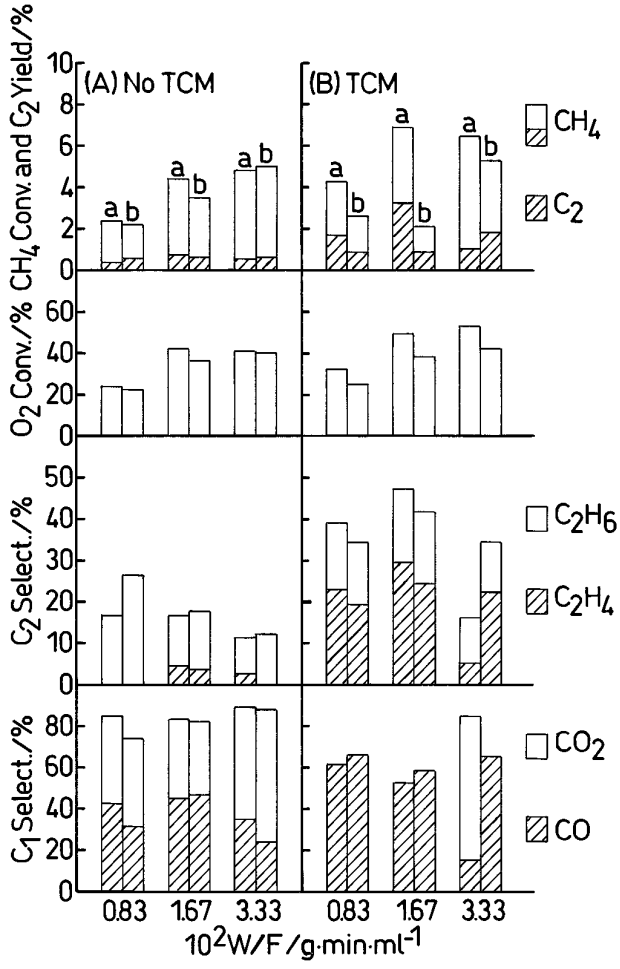

FIG. 12. Effects of the space time (*W*/*F*) on the oxidation of methane in the absence (A) and presence (B) of TCM on $Sr_3(PO_4)_2$ at 973 K. Pretreatment and reaction conditions: same as those in Fig. 3 except weight of the catalyst.

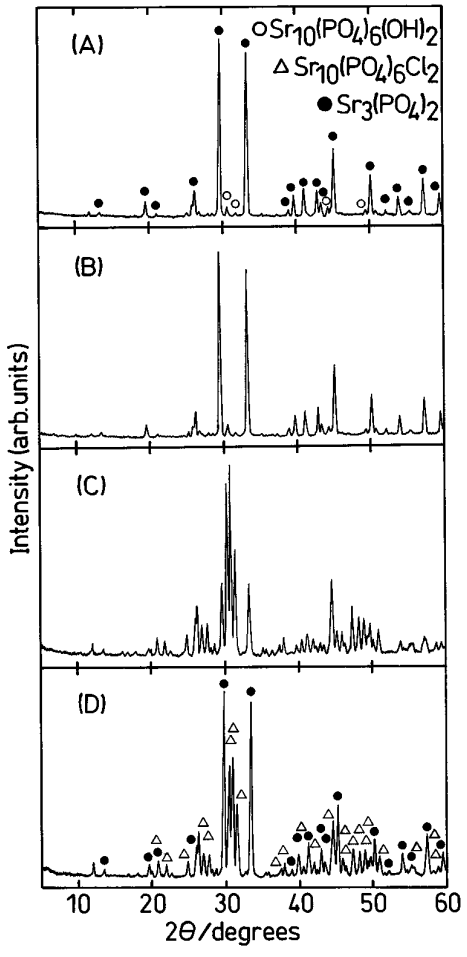

FIG. 13. XRD patterns of the catalysts used in the oxidation of methane in the absence and presence of TCM on $Sr_3(PO_4)_2$. (A), (B), (C), and (D): Catalysts previously employed in obtaining results reported in Fig. 12 at $W/F = 0.83 \times 10^{-2}$ and 3.33×10^{-2} g · min · ml^{-1} in the absence ((A) and (B), respectively) and presence of TCM ((C) and (D), respectively), but after 6 h on stream.

the lower W/F (Fig. 13). Since both the hydroxyapatite and the phosphate can be converted to the chlorapatite in the presence of TCM it is evident that the propensity of the hydroxyapatite to convert to the phosphate at the temperatures employed in the present work has less influence on the results from the methane reaction than originally anticipated.

CONCLUSIONS

1. The catalytic activity of SrHAp for the oxidation of methane exceeds that of CaHAp with and without TCM.

2. At the temperatures employed in the present work SrHAp is, at least in part, converted to $Sr_3(PO_4)_2$. The extent of this conversion appears to be dependent on Sr/P with the maximum occurring for the stoichiometric apatite. The conversion appears to require a temperature higher than 873 K.

3. In the presence of TCM the hydroxyapatite is partially converted to chlorapatite rather than the phosphate.

4. In the presence of TCM the selectivities to CO and to C_2H_4 are increased on SrHAp particularly so with increase in time-on-stream. Since the conversion of hydroxyapatite to chlorapatite presumably increases with time-on-stream the increased selectivities appear to be related to the formation of the chlorinated compound.

5. The presence of chlorapatite apparently suppresses the further oxidation of CO and C_2H_4.

ACKNOWLEDGMENTS

The financial support provided by a ''Grant for Natural Gas Research'' from The Japan Petroleum Institute to S.S. and by the Natural Sciences and Engineering Research Council of Canada to J.B.M. is gratefully acknowledged.

REFERENCES

1. J. S. Lee and S. T. Oyama, *Catal. Rev.-Sci. Eng.* **30,** 249 (1988).
2. Y. Amenomiya, V. I. Birss, M. Goledzinowski, J. Galuszka, and A. R. Sanger, *Catal. Rev.-Sci. Eng.* **32,** 163 (1990).
3. A. M. Maitra, *Appl. Catal. A.* **35,** 169 (1993).
4. J. M. Fox, *Catal. Rev.-Sci. Eng.* **35,** 169 (1993).
5. J. H. Lunsford, *Angew. Chem. Int. Ed. Engl.* **34,** 970 (1995).
6. T. J. Hall, J. S. J. Hargreaves, G. J. Hutchings, R. W. Joyner, and S. H. Taylor, *Fuel Process. Technol.* **42,** 151 (1995).
7. A. T. Ashcroft, A. K. Cheetham, J. S. Foord, M. L. H. Green, C. P. Grey, A. J. Murrell, and P. D. F. Vernon, *Nature* **344,** 319 (1990).
8. K. Kunimori, S. Umeda, J. Nakamura, and T. Uchijima, *Bull. Chem. Soc. Jpn.* **65,** 2562.
9. J. Nakamura, S. Umeda, K. Kubushiro, K. Kunimori, and T. Uchijima, *Sekiyu Gakkaishi* **36,** 97 (1993).
10. S. Ahmed and J. B. Moffat, *Catal. Lett.* **1,** 141 (1988).
11. T. Ohno and J. B. Moffat, *Appl. Catal. A.* **93,** 141 (1993).
12. S. Sugiyama and Moffat, J. B., *Energy Fuels* **7,** 279 (1993).
13. S. Sugiyama and J.B. Moffat, J.B., *Energy Fuels,* **8,** 463 (1994).
14. R. Voyatzis and J. B. Moffat, *Energy Fuels* **8,** 1106 (1994).
15. R. Voyatzis and J. B. Moffat, *Energy Fuels* **9,** 240 (1995).
16. S. Ahmed and J. B. Moffat, *Chem. Eng. Technol.* **18,** 132 (1995).
17. S. Sugiyama, T. Miyamoto, H. Hayashi, and J. B. Moffat, *Bull. Chem. Soc. Jpn.* **69,** 235 (1996).
18. S. Sugiyama, T. Minami, H. Hayashi, M. Tanaka, N. Shigemoto, and J. B. Moffat, *J. Chem. Soc. Faraday Trans.* **92,** 293 (1996).
19. S. Sugiyama, T. Minami, T. Moriga, H. Hayashi, K. Koto, M. Tanaka, and J. B. Moffat, *J. Mater. Chem.* **6,** 459 (1996).
20. S. Sugiyama, T. Minami, H. Hayashi, M. Tanaka, N. Shigemoto, and J. B. Moffat, *Energy Fuels* **10,** 828 (1996).
21. J. A. S. Bett, L. G. Christner, and W. K. Hall, *J. Catal.* **13,** 332 (1969).
22. C. L. Kibby and W. K. Hall, *J. Catal.* **29,** 144 (1973).
23. C. L. Kibby and W. K. Hall, *J. Catal.* **31,** 65 (1973).
24. H. Monma, *J. Catal.* **75,** 200 (1982).
25. Y. Imizu, M. Kadoya, H. Abe, H. Ito, and A. Tada, *Chem. Lett.* 415 (1982).
26. Y. Izumi, S. Sato, and K. Urabe, *Chem. Lett.* 1646 (1983).

27. Y. Matsumura and J. B. Moffat, *Catal. Lett.* **17,** 197 (1993).
28. Y. Matsumura and J. B. Moffat, *J. Catal.* **148,** 323 (1994).
29. Y. Matsumura, S. Sugiyama, H. Hayashi, N. Shigemoto, K. Saitoh, and J. B. Moffat, *J. Mol. Catal.* **92,** 81 (1994).
30. Y. Matsumura, J. B. Moffat, S. Sugiyama, H. Hayashi, N. Shigemoto, and K. Saitoh, *J. Chem. Soc., Faraday Trans.* **90,** 2133 (1994).
31. Y. Matsumura, S. Sugiyama, H. Hayashi, and J. B. Moffat, *J. Solid State Chem.* **114,** 138 (1995).
32. Y. Matsumura, S. Sugiyama, H. Hayashi, and J. B. Moffat, *Catal. Lett.* **30,** 235 (1995).
33. E. Hayek and H. Newesely, *Inorg. Synth.* **7,** 63 (1963).
34. R. Klement, *Z. Anorg. Allg. Chem.* **242,** 215 (1939).
35. T. Kanazawa and H. Monma, ''Shin-jikken Kagaku (in Japanese),'' Vol. 8, No. 2, p. 622. Chemical Society of Japan, Maruzen, Tokyo, 1977.
36. H. V. Tartar and J. R. Lorah, *J. Am. Chem. Soc.* **51,** 1091 (1929).
37. B. O. Fowler, *Inorg. Chem.* **13,** 207 (1974).
38. H. Monma, *Shokubai* (in Japanese, *Catalysts and Catalysis*) **27,** 237 (1985).
39. S. Muramatsu, C. Kato, K. Fujita, and K. Matsuda, *Nippon Kagaku Kaishi*, 531 (1994).
40. H. Monma, S. Ueno, and T. Kanazawa, *J. Chem. Tech. Biotechnol.* **31,** 15 (1981).
41. J. A. Bett, L. G. Christner, and W. K. Hall, *J. Am. Chem. Soc.* **89,** 5535 (1967).